

# Espartaco 2, a New Stellar Spectrograph at Universidad de los Andes

B. Oostra<sup>1</sup> and M. G. Batista<sup>1</sup>

<sup>1</sup>Universidad de los Andes, Departamento de Física, Carrera 1 #18a - 12, 111711, Bogotá, Colombia.

**Keywords:** *astronomical instrumentation, stars: radial velocity, stars: spectroscopy, astronomy education*

## Abstract

We present the construction and early results of ESPARTACO 2, a new stellar spectrograph built for research and education at the Astronomical Observatory of the Universidad de los Andes in Bogotá, Colombia. This instrument offers several resolution modes, from 20,000 in the first order using a 50  $\mu\text{m}$  fiber, to 100,000 in the second order in the near-infrared. Precise radial-velocity measurements were made possible by simultaneous wavelength calibration. Combined with the 40-cm Meade telescope located at our facilities, a limiting magnitude of 6 was achieved. This instrument represents a significant improvement over its predecessor in terms of throughput, reliability, and ease of use.

## Resumen

Presentamos la construcción y los primeros resultados de ESPARTACO 2, el nuevo espectrógrafo estelar que fue construido con fines educativos y de investigación en el Observatorio Astronómico de la Universidad de los Andes en Bogotá, Colombia. Este instrumento tiene la capacidad de ofrecer varias resoluciones, desde 20,000 cuando se usa la fibra de 50  $\mu\text{m}$  en primer orden, hasta 100,000 en el segundo orden en el infrarrojo cercano. Es posible realizar medidas precisas de velocidad radial estelar mediante la calibración simultánea en longitud de onda. Al combinarse con el telescopio Meade de 40 cm localizado en nuestras instalaciones, se logra estudiar objetos hasta magnitud de 6. Este instrumento representa una mejora respecto a su antecesor en cuanto a su eficiencia lumínica, fiabilidad y facilidad de uso.

**Corresponding author:** B. Oostra *E-mail address:* [boostra@uniandes.edu.co](mailto:boostra@uniandes.edu.co)  
**Received:** April 29, 2024 **Accepted:** April 21, 2025

## 1. Introduction

Our campus observatory arose from the need to make observations that could complement theoretical astronomy courses. Our location near Bogotá's city center has some drawbacks, such as light pollution, severe seeing, and highly variable weather, but the advantage is that we can seize the opportunity when the conditions are good.

In this urban environment, high-resolution spectroscopy of the sun and bright stars is more promising than any other astronomical technique and has proven to be a fruitful endeavor (Oostra, 2012, 2017; Oostra & Batista, 2024) through 15 years of work with *ESPARTACO*, *Espectrógrafo de Alta Resolución para Trabajos Astronómicos en Colombia* (Oostra & Ramírez, 2011). This instrument is a high-resolution, low-cost spectrograph designed for undergraduate research projects. Pursuing this path, half a dozen spectrographs have been built and used at our observatory over the past three decades.

Despite achieving all the goals, ESPARTACO has several issues. It was built in 2007 with a non-optimal design using

parts that were available at the time; the mismatch between these components produced a very low throughput. Moreover, wavelength calibration spectra must be taken before or after the science spectra, mechanical stability is deficient, and proper focusing is challenging.

Despite its difficulties, ESPARTACO has provided valuable experience in astronomical studies and atomic physics laboratory work. This justified some investment in more optimized optical components, prompting the construction of a new instrument, which began in 2018 and was completed in 2023. Building instruments locally is a way to reduce costs, but it also provides experience in astronomical instrumentation design. In § 2, we provide a technical description of the instrument. In § 3, we present the results of the quality tests. Finally, in § 4 we list our conclusions.

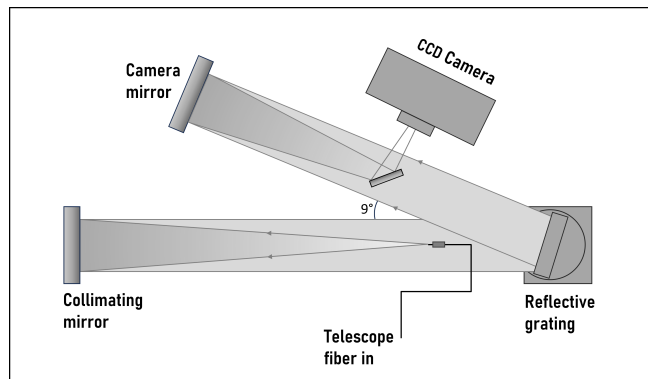


**Figure 1.** Optical layout of ESPARTACO 2. The angle between the collimator and camera is  $9^\circ$ . The only moving parts are the grating, which can rotate  $360^\circ$ , and the fiber support.

## 2. Description of the instrument

### 2.1. Optical layout

ESPARTACO 2 is a Czerny-Turner spectrograph with on-axis parabolic mirrors of 15 cm diameter. The grating is 14 cm wide and 12 cm high, with a density of 1200 grooves/mm and no blaze. The lengths of the collimator and camera mirror were 120 cm (F/8) and 76 cm (F/5), respectively. The instrument can be used in the first and second diffraction orders, as shown in Figure 1.

### 2.2. Fibers

The instrument is fed via four optical fibers of circular cross-section: three of  $50\ \mu\text{m}$  diameter and one of  $10\ \mu\text{m}$ . At the collimator end of these fibers, their tips were polished without ferrules to minimize the spacing between them. Their plastic sleeves kept the cores 0.9 mm apart, which placed the images in the camera at a vertical spacing of 63 pixels. The exit beam of these fibers was wider than that of the F/8 collimator, resulting in luminosity loss. The multiplicity of fibers makes it possible to simultaneously register the calibration spectrum on the same image as the stellar spectrum; this is necessary for precise measurements of radial velocities and was not possible with the previous spectrograph. For stellar observations, one  $50\ \mu\text{m}$  fiber carries the light from the star, another carries the light from a Th-Ar hollow-cathode lamp, and a third may be coupled to a neon lamp for eventual fast position or focus checks. A small horizontal offset exists between any pair of fibers, which must be measured empirically. The star fiber is coupled to the telescope via an interface from Shelyak Instruments<sup>1</sup>.

<sup>1</sup>In order to reduce the size of the stellar image in the telescope's focal plane, and thus maximize the amount of light through the optical fiber, we connect to the telescope a Meade Electronic Micro-Focuser, Meade series 4000 f/6.3 focal reducer and the Shelyak FIGU (Fiber Injection and Guiding Unit) to inject the starlight into an optical fiber and a guiding camera.

### 2.3. Camera

The camera is a Kodak KAF1603ME CCD array of  $1530 \times 1020$  pixels measuring  $9\ \mu\text{m}$  square. It is commonly operated at  $-15^\circ\text{C}$ . Downloading images using a USB cable takes only a few seconds. The technical specifications are as follows:

- Full well = 100,000 electrons, converted to 65535 ADU, give a gain of 1.52 e/ADU
- Read-out noise: 10.5 ADU (RMS) = 16 electrons.
- Dark current (reported): 1 electron per pixel per second at  $0^\circ\text{C}$
- Dark current (measured): 1 electron per pixel per minute at  $-15^\circ\text{C}$
- Quantum Efficiency: 75% at H- $\alpha$ , 50% at H- $\beta$ .
- Sensitivity range: 400 - 800 nm.

### 2.4. Structure

The optical components are mounted in a rigid  $165 \times 45 \times 35$  cm steel frame made of a 50-mm-wide steel angle covered with black acrylic panes. The only moving parts are the grating's support, which can rotate  $360^\circ$ , and the fiber support which can travel 2 cm for focusing. Both devices are driven by small stepper motors that are controlled manually. The angular position of the grating is monitored using a webcam. The stepper motors and controlling webcam are important improvements over the previous version of ESPARTACO 1 (Oostra & Ramírez, 2011).

### 2.5. Thermal instability

A major problem is the lack of a thermally stabilized room for the spectrographs. The instrument is located in the small dome building where the temperature may change from below  $10^\circ\text{C}$  at 3:00 a.m. to more than  $20^\circ\text{C}$  at 3:00 p.m. This necessitates an adjustment of the focus. However, extreme refocusing degrades the spectral line profile; therefore, we attempted to mitigate thermal changes using insulation (20 mm Ethafoam) and a low-power internal heating system.

## 3. Results

### 3.1. Resolution

To assess the resolution of the spectrograph, we performed a series of linewidth measurements on carefully focused spectra of our Th-Ar lamp. We used only thorium lines because they are perceptibly narrower than argon lines, possibly because of the greater atomic mass, which reduces Doppler broadening.

The measurements were made using the same  $50\ \mu\text{m}$  fibre that is commonly employed for stars.

For each profile, we adjusted a Gaussian fit to four or five central data points. The reported line widths are the FWHM of these fits. Each selected Th line was measured in the first and second orders.

Figures 2, 3, and 4 show the theoretical and measured line widths, theoretical dispersion, and theoretical and

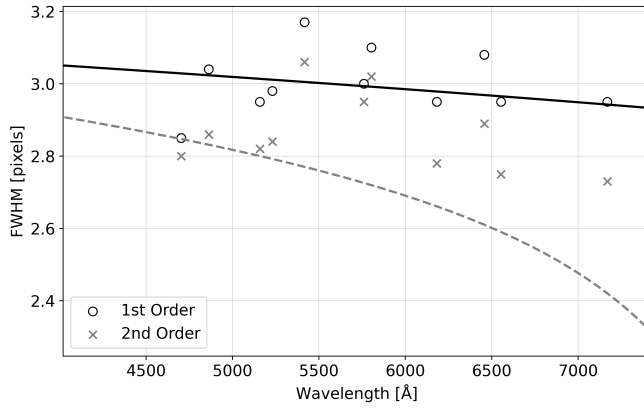


**Figure 2.** Measured widths of Th emission lines. The circles and crosses represent the first- and second-order measurements, respectively. Theoretical line widths are shown with solid line for the first order and dashed for second order.

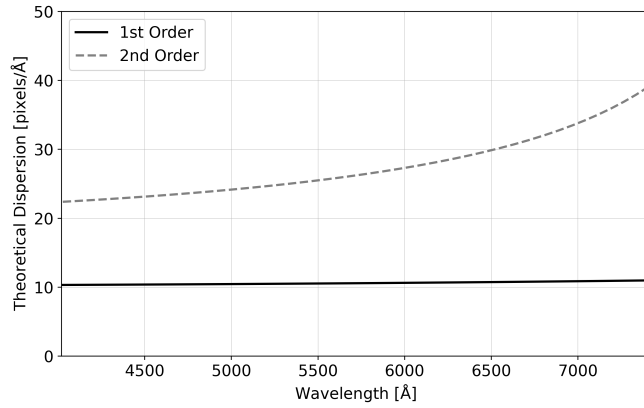


**Figure 3.** Theoretical dispersion of the spectrograph. The solid and dashed lines represent the first and second orders, respectively. Observed values are found to agree with the theory.

measured resolutions, respectively. For the calculations, we included only geometrical optics, no diffraction, and instead of a circular input, we assumed a rectangular entrance slit of  $45 \mu\text{m}$ . As can be seen, stars must be observed at a resolution of 20,000 in the first order, which is considerably less than the 31,000 given by our previous spectrograph.

Through the narrow  $10 \mu\text{m}$  fibre we took some images of the particularly strong Th 5761 line. In the first order, a width of 2.03 pixels can be readily measured, suggesting that this fiber enhances the resolution by approximately 50% for bright emission lines in the first order. In the second order, the focusing is very ambiguous and the results are unclear. In several images, it was possible to fit a Gaussian to the three central points and obtain a width of 1.8 or 1.9 pixels; however, a large amount of light was scattered outside this peak. This indicates that the diffraction effects are not negligible. A line width below the Nyquist limit of 2 pixels is not useful.

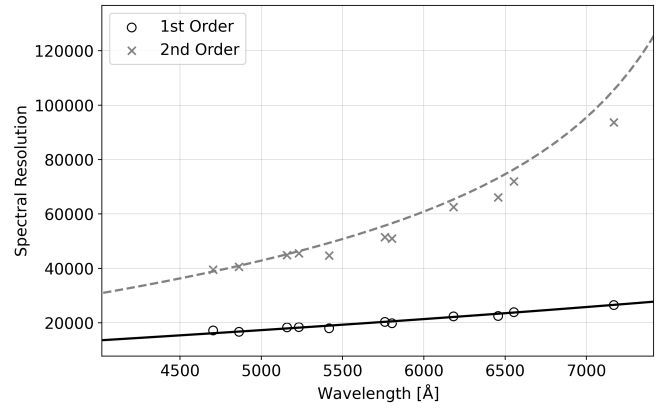


**Figure 4.** Spectral resolution computed from dispersion and line width. Conventions as before.

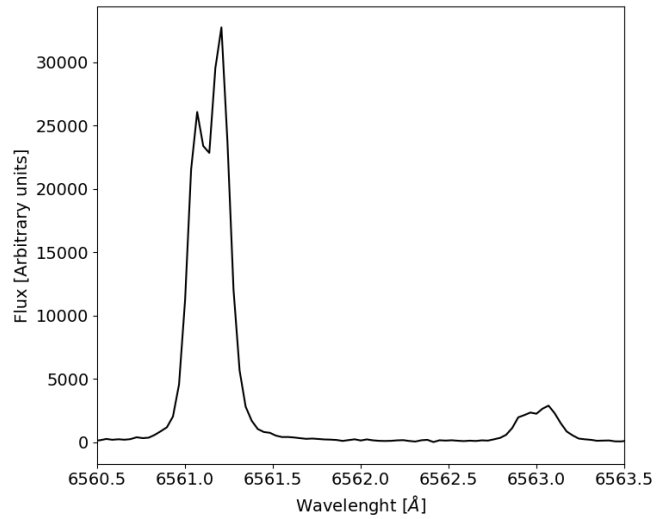


**Figure 5.** Spectrum of deuterium- $\alpha$  and its fine structure, obtained with 20 seconds of exposure using the  $10 \mu\text{m}$  fiber in the second order (left). A trace of normal hydrogen, which was present in the deuterium tube, produced a small emission line on the right side. The isotopic shift constitutes regular assignments for students. For this experiment, deuterium is better than normal hydrogen because it has less thermal broadening.

The light transmitted by the  $10\text{-}\mu\text{m}$  fiber is very weak, and the exposure times are prohibitively long. In contrast, continuous spectra through this fiber are modulated by intermodal interference (Hlubina, 1999; Baudrand & Walker, 2001; Lemke et al., 2011). Nevertheless, laboratory spectra are useful for studying the Zeeman effect and fine structure of deuterium (Figure 5).

### 3.2. Throughput and limiting magnitude around H-alpha

The main improvement of ESPARTACO 2 over our previous spectrograph is the gain in luminosity, which was also the main reason for constructing the new instrument. The new spectrograph has 14 times greater optical throughput than its forerunner, as measured by aperture photometry of neon

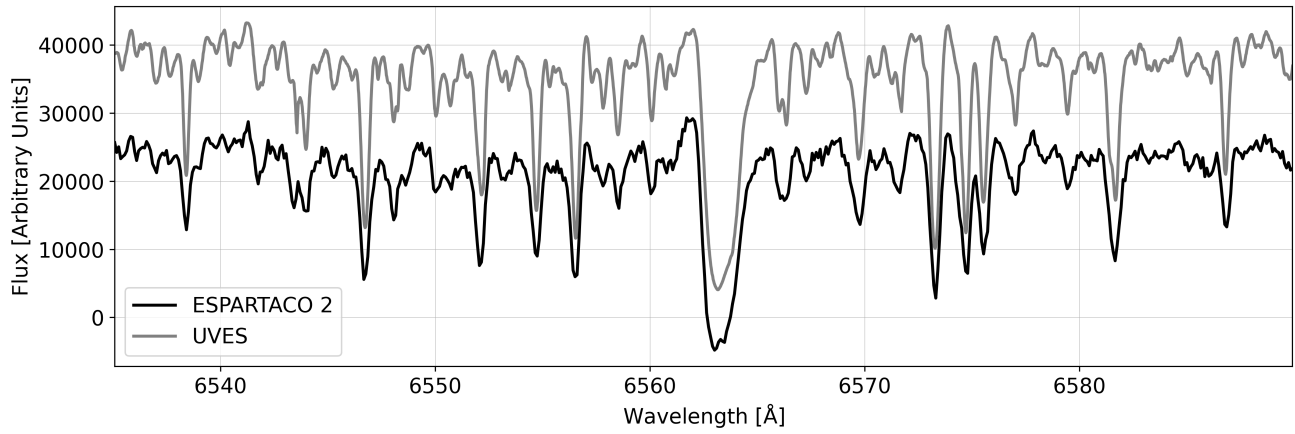


**Figure 6.** Spectrum of HD49331 obtained with ESPARTACO 2 (black line); for comparison, the same spectrum from UVES (grey line), at resolution 80000; (Bagnulo et al., 2003).

spectra. This represents a progress of almost three stellar magnitudes and is mainly due to the size of the new grating,  $120 \times 140$  mm, compared with the old grating's  $50 \times 50$  mm.

The limiting magnitude depends on the stellar spectral type and observed wavelength range. If we define the limit by an S/N ratio of 10 and an exposure time of 20 min on our 40-cm telescope, the limiting V magnitude is approximately 5 for early type stars and 6 for late-type stars observed at H-alpha in first order. As an example, Figure 6 shows the spectrum of HD49331, a red supergiant of magnitude  $V = 5.1$ , obtained with a 20-minute exposure and giving a signal-to-noise ratio of 38.

Figure 6 compares our spectrum of HD49331 with a spectrum of the same star recorded at a resolution of 80.000 by the UVES spectrograph and published under the Paranal Observatory Project (Bagnulo et al., 2003). The comparison shows that the main features are clearly legible in our data, and many smaller features are missing because of the lower resolution and signal strength.

In addition to the Sun, we can study some bright stars in the second order. Figure 7 shows the second-order spectrum of Betelgeuse obtained in a 10-minute exposure. In this configuration, the higher resolution allowed some line width measurements, and the results are shown in Table 1. The most conspicuous feature is that stellar lines are broader than telluric lines because of the turbulence and rotation of the star. This distinction is not visible in Figure 6, partly due to the lower resolution at first order and because HD 49331 is less turbulent.

Second-order spectra have the disadvantage that they span a range of only  $50 \text{ Å}$ , whereas first-order spectra cover  $140 \text{ Å}$ . Moreover, the exposure times must be long, and the limiting magnitude is approximately 1. This option is particularly useful for solar and laboratory studies.

### 3.3. Budget

All optical components were purchased from the market. The 15-cm mirrors and supports were obtained from

**Table 1.** Prominent absorption lines in the Betelgeuse spectrum

#	$\lambda$ obs [Å]	Species	Width [Å]	$\lambda$ rest [Å]	RV [km/s]
1	6543.91	H <sub>2</sub> O	0.15	6543.907	0.14
2	6547.21	Fe+Ti	0.48	6546.253	43.86
3	6548.62	H <sub>2</sub> O	0.18	6548.622	-0.09
4	6552.63	H <sub>2</sub> O	0.22	6552.629	0.05
5	6555.16	Ti	0.52	6554.223	42.89
6	6557.03	Ti	0.57	6556.062	44.30
7	6570.20	Fe+Fe	0.65	6569.215	45.00
8	6572.08	H <sub>2</sub> O	0.18	6572.086	-0.27
9	6573.71	Ca	0.65	6572.779	42.49

Edmund Optics, as well as the diagonal mirror. Both motor stages were obtained from Optimal Engineering Systems Inc. (OES). The grating was obtained from Horiba Jobin-Yvon. The camera was obtained from SBIG (taken over by Diffraction Limited). The prices of these components add up to approximately 17000 USD.

The structural frame, mounting for the diagonal mirror, and other parts were built at our Physics Department Mechanics Laboratory. Optical fibers and other hardware were purchased at a low cost from local markets. We believe that the overall cost/benefit ratio is reasonable, considering that our environmental conditions do not justify the use of expensive equipment for monitoring.

## 4. Final remarks

ESPARTACO 2 will be useful for research and teaching from high school to graduate level. This instrument has the capacity to offer several resolutions, depending on the order and diameter of the optical fiber used, has a greater luminous throughput, and the advantage of moving parts

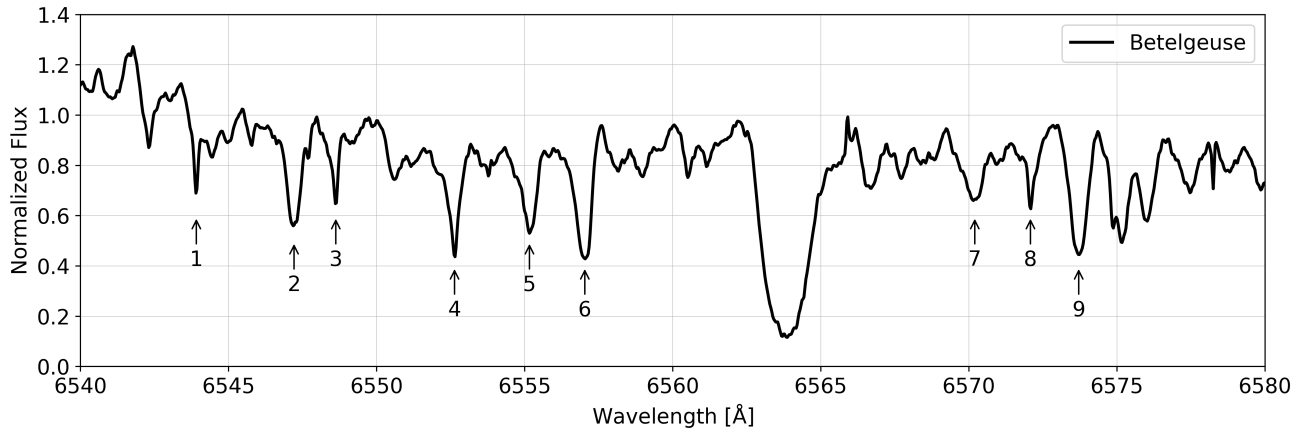


**Figure 7.** Spectrum of Betelgeuse obtained with ESPARTACO 2 in second order in a 10-minute exposure. Numbers 1–9 indicate the selected absorption lines discussed in the text (Table 1). In particular, lines 1, 3, 4 and 8 are telluric  $\text{H}_2\text{O}$  lines, and are evidently narrower than the stellar lines; this distinction is not visible in the first-order spectrum shown in Figure 6.

with stepper motors, delivering considerable improvements over its predecessor. However, eventual refinements and reforms may be implemented in the future to address these issues.

- Add another  $50\ \mu\text{m}$  fiber with a micro-lens in order to couple the fiber optimally to the collimator aperture. This would increase the limiting magnitude, albeit at lower spectral resolutions.
- Install a chiller for water-cooling the camera.
- Couple the focus motor and heating system to a thermostat.
- Implement digital encoders for the position of the grating and the focus motor.
- Replace the mirrors by off-axis paraboloids, which would eliminate the diagonal mirror and place the fibers outside the collimator beam, enhancing the image quality and luminosity.

## References

- Bagnulo, S., Jehin, E., Ledoux, C., et al. 2003, *Msngr*, 114, 10
- Baudrand, J., & Walker, G. A. 2001, *PASP*, 113, 851, doi: [10.1086/322143](https://doi.org/10.1086/322143)
- Hlubina, P. 1999, *JMOp*, 46, 1595, doi: [10.1080/09500349908231358](https://doi.org/10.1080/09500349908231358)
- Lemke, U., Corbett, J., Allington-Smith, J., & Murray, G. 2011, *MNRAS*, 417, 689, doi: [10.1111/j.1365-2966.2011.19312.x](https://doi.org/10.1111/j.1365-2966.2011.19312.x)
- Oostra, B. 2012, *AmJPh*, 80, 363, doi: [10.1119/1.3684841](https://doi.org/10.1119/1.3684841)
- . 2017, *AmJPh*, 85, 295, doi: [10.1119/1.4975109](https://doi.org/10.1119/1.4975109)
- Oostra, B., & Batista, M. G. 2024, *RMxAA*, 60, 367, doi: [10.22201/ia.01851101p.2024.60.02.14](https://doi.org/10.22201/ia.01851101p.2024.60.02.14)
- Oostra, B., & Ramírez, D. 2011, *Revista Colombiana de Física*, 43(2), 312